ELectronics EXpress

LETTER

IEICE Electronics Express, Vol.14, No.3, 1–9

Single-end-access strain and temperature sensing based on multimodal interference in polymer optical fibers

Tomohito Kawa[1], Goki Numata[1], Heeyoung Lee[1], Neisei Hayashi[2], Yosuke Mizuno[1a)], and Kentaro Nakamura[1]

[1] *Institute of Innovative Research, Tokyo Institute of Technology, Yokohama 226–8503, Japan*

[2] *Research Center for Advanced Science and Technology, The University of Tokyo, Tokyo 153–8904, Japan*

a) *ymizuno@sonic.pi.titech.ac.jp*

Abstract: We develop a single-end-access strain/temperature sensor configuration based on multimodal interference in a polymer optical fiber (POF) with an extremely high sensitivity. The light Fresnel-reflected at the distal open end of the POF is exploited. We obtain high strain and temperature sensitivities of –122.2 pm/με and 10.1 nm/°C, respectively, which are shown to be comparable to those in two-end-access configurations.

Keywords: optical fiber sensors, multimodal interference

Classification: Optical systems

References

[1] A. D. Kersey, *et al.*: "Fiber grating sensors," J. Lightwave Technol. **15** (1997) 1442 (DOI: 10.1109/50.618377).

[2] J. Jung, *et al.*: "Fiber Bragg grating temperature sensor with controllable sensitivity," Appl. Opt. **38** (1999) 2752 (DOI: 10.1364/AO.38.002752).

[3] B. O. Guan, *et al.*: "Simultaneous strain and temperature measurement using a superstructure fiber Bragg grating," IEEE Photonics Technol. Lett. **12** (2000) 675 (DOI: 10.1109/68.849081).

[4] Y. Zhang and W. Yang: "Simultaneous precision measurement of high temperature and large strain based on twisted FBG considering nonlinearity and uncertainty," Sens. Actuators A Phys. **239** (2016) 185 (DOI: 10.1016/j.sna.2016.01.012).

[5] V. Bhatia and A. M. Vangsarkar: "Optical fiber long-period grating sensors," Opt. Lett. **21** (1996) 692 (DOI: 10.1364/OL.21.000692).

[6] Y. P. Wang, *et al.*: "Highly sensitive long-period fiber-grating strain sensor with low temperature sensitivity," Opt. Lett. **31** (2006) 3414 (DOI: 10.1364/OL.31.003414).

[7] P. Wang, *et al.*: "Fabrication of phase-shifted long-period fiber grating and its application to strain measurement," IEEE Photonics Technol. Lett. **27** (2015) 557 (DOI: 10.1109/LPT.2014.2385067).

[8] T. Kurashima, *et al.*: "Brillouin optical-fiber time domain reflectometry," IEICE Trans. Commun. **E76-B** (1993) 382.

[9] Y. Dong, *et al.*: "High-spatial-resolution fast BOTDA for dynamic strain

DOI: 10.1587/elex.14.20161239
Received December 14, 2016
Accepted December 16, 2016
Publicized January 13, 2017
Copyedited February 10, 2017

measurement based on differential double-pulse and second-order sideband of modulation," IEEE Photon. J. **5** (2013) 2600407 (DOI: 10.1109/JPHOT.2013.2267532).
[10] D. Garus, *et al.*: "Distributed sensing technique based on Brillouin optical-fiber frequency-domain analysis," Opt. Lett. **21** (1996) 1402 (DOI: 10.1364/OL.21.001402).
[11] K. Hotate and T. Hasegawa: "Brillouin optical-fiber time domain reflectometry," IEICE Trans. Electron. **E83-C** (2000) 405.
[12] Y. Mizuno, *et al.*: "Proposal of Brillouin optical correlation-domain reflectometry (BOCDR)," Opt. Express **16** (2008) 12148 (DOI: 10.1364/OE.16.012148).
[13] Y. Mizuno, *et al.*: "Ultrahigh-speed distributed Brillouin reflectometry," Light Sci. Appl. **5** (2016) e16184 (DOI: 10.1038/lsa.2016.184).
[14] M. A. Farahani and T. Gogolla: "Spontaneous Raman scattering in optical fibers with modulated probe light for distributed temperature Raman remote sensing," J. Lightwave Technol. **17** (1999) 1379 (DOI: 10.1109/50.779159).
[15] M. N. Alahbabi, *et al.*: "Simultaneous temperature and strain measurement with combined spontaneous Raman and Brillouin scattering," Opt. Lett. **30** (2005) 1276 (DOI: 10.1364/OL.30.001276).
[16] M. K. Saxena, *et al.*: "Raman optical fiber distributed temperature sensor using wavelet transform based simplified signal processing of Raman backscattered signals," Opt. Laser Technol. **65** (2015) 14 (DOI: 10.1016/j.optlastec.2014.06.012).
[17] Y. J. Rao, *et al.*: "Dual-cavity interferometric wavelength-shift detection for in-fiber Bragg grating sensors," Opt. Lett. **21** (1996) 1556 (DOI: 10.1364/OL.21.001556).
[18] O. Frazão, *et al.*: "Optical fiber refractometry based on multimode interference," Appl. Opt. **50** (2011) E184 (DOI: 10.1364/AO.50.00E184).
[19] Y. Liu and L. Wei: "Low-cost high-sensitivity strain and temperature sensing using graded-index multimode fibers," Appl. Opt. **46** (2007) 2516 (DOI: 10.1364/AO.46.002516).
[20] S. M. Tripathi, *et al.*: "Strain and temperature sensing characteristics of single-mode–multimode–single-mode structures," J. Lightwave Technol. **27** (2009) 2348 (DOI: 10.1109/JLT.2008.2008820).
[21] J. Huang, *et al.*: "Polymer optical fiber for large strain measurement based on multimode interference," Opt. Lett. **37** (2012) 4308 (DOI: 10.1364/OL.37.004308).
[22] G. Numata, *et al.*: "Ultra-sensitive strain and temperature sensing based on modal interference in perfluorinated polymer optical fibers," IEEE Photon. J. **6** (2014) 6802306 (DOI: 10.1109/JPHOT.2014.2352637).
[23] G. Numata, *et al.*: "Strain and temperature sensing based on multimode interference in partially chlorinated polymer optical fibers," IEICE Electron. Express **12** (2015) 20141173 (DOI: 10.1587/elex.12.20141173).
[24] G. Numata, *et al.*: "Drastic sensitivity enhancement of temperature sensing based on multimodal interference in polymer optical fibers," Appl. Phys. Express **8** (2015) 072502 (DOI: 10.7567/APEX.8.072502).
[25] A. Kumar, *et al.*: "Transmission characteristics of SMS fiber optic sensor structures," Opt. Commun. **219** (2003) 215 (DOI: 10.1016/S0030-4018(03)01289-6).
[26] M. Kumar, *et al.*: "A comparison of temperature sensing characteristics of SMS structures using step and graded index multimode fibers," Opt. Commun. **312** (2014) 222 (DOI: 10.1016/j.optcom.2013.09.034).
[27] A. Mehta, *et al.*: "Multimode interference-based fiber-optic displacement sensor," IEEE Photonics Technol. Lett. **15** (2003) 1129 (DOI: 10.1109/LPT.

DOI: 10.1587/elex.14.20161239
Received December 14, 2016
Accepted December 16, 2016
Publicized January 13, 2017
Copyedited February 10, 2017

2003.815338).
[28] E. Li, *et al.*: "Fiber-optic temperature sensor based on interference of selective higher-order modes," Appl. Phys. Lett. **89** (2006) 091119 (DOI: 10.1063/1.2344835).
[29] R. M. Ribeiro and M. M. Werneck: "An intrinsic graded-index multimode optical fibre strain-gauge," Sens. Actuators A **111** (2004) 210 (DOI: 10.1016/j.sna.2003.11.009).
[30] Y. Koike and M. Asai: "The future of plastic optical fiber," NPG Asia Mater. **1** (2009) 22 (DOI: 10.1038/asiamat.2009.2).
[31] T. Ishigure, *et al.*: "Optimum index profile of the perfluorinated polymer-based GI polymer optical fiber and its dispersion properties," J. Lightwave Technol. **18** (2000) 178 (DOI: 10.1109/50.822790).
[32] Y. Mizuno and K. Nakamura: "Experimental study of Brillouin scattering in perfluorinated polymer optical fiber at telecommunication wavelength," Appl. Phys. Lett. **97** (2010) 021103 (DOI: 10.1063/1.3463038).

1 Introduction

Fiber-optic strain and temperature sensors have been developed based on a variety of principles including fiber Bragg gratings [1, 2, 3, 4], long-period gratings [5, 6, 7], Brillouin scattering [8, 9, 10, 11, 12, 13], Raman scattering [14, 15, 16], and optical interference [17, 18, 19, 20, 21, 22, 23, 24, 25, 26]. While many types of interference-based strain and temperature sensors are reported, those based on the interference of multiple guided modes in multimode fibers (MMFs) have received a great deal of attention for the past two decades because of their system simplicity, cost efficiency, and high sensitivity. As summarized in Table 1 in Ref. [18], a number of configurations have been implemented; the most commonly used configuration of them is a so-called "single-mode-multimode-single-mode" (SMS) structure [19, 20, 21, 22, 23, 24, 25, 26], where an MMF is sandwiched between two single-mode fibers (SMFs).

Let us review the recent developments of SMS-based strain and temperature sensors. Using a 1.8-m-long silica graded-index (GI-) MMF, a strain sensitivity of +18.6 pm/με and a temperature sensitivity of +58.5 pm/°C were obtained at 1550 nm [19]. Both the absolute values and the signs of the strain and temperature sensitivities were found to be determined by "critical wavelengths" [20], which depend on the core diameter and/or the dopant of silica MMFs. To extend the measurable strain range, using a 0.16-m-long polymethyl methacrylate (PMMA)-based step-index polymer optical fiber (POF) as an MMF, a strain sensitivity of −1.72 pm/με and a temperature sensitivity of −56.8 pm/°C were obtained at 1570 nm [21]. However, the propagation loss of PMMA-based POFs at telecom wavelength is so high ($\gg 1 \times 10^5$ dB/km) that the measurable distance is intrinsically limited to several meters or less. To overcome this problem, we have recently implemented SMS-based strain and temperature sensors using perfluorinated (PF) GI-POFs [22, 23, 24], which are the only POFs with a relatively low loss of ~250 dB/km even at 1550 nm (or ~50 dB/km at 1300 nm). When the POF length was 1.0 m and the core diameter was 62.5 μm, we obtained a strain sensitivity of −111.8 pm/με and a temperature sensitivity of +49.8 nm/°C at room temperature

DOI: 10.1587/elex.14.20161239
Received December 14, 2016
Accepted December 16, 2016
Publicized January 13, 2017
Copyedited February 10, 2017

at 1300 nm; these values are by far larger than those previously reported using other MMFs [22].

Thus, substantial efforts have been made to improve the performance of SMS-based strain and temperature sensors, but almost all the SMS-based sensors reported thus far are two-end-access systems, in which both ends of the MMF are physically connected to SMFs. From a practical viewpoint, single-end-access configurations with an enhanced degree of freedom in embedding the sensors into structures are preferable. There are only three examples of such single-end-access configurations; the first is a displacement sensor reported by Mehta et al. [27], which comprises an SMF-MMF-airgap-mirror structure. It is, however, difficult to directly employ this structure to measure strain and temperature; in addition, use of the mirror reduces the ease of handling. The second is a temperature sensor reported by Li et al. [28], in which no descriptions on strain sensing capability have been provided at all. The third is a strain sensor reported by Ribeiro et al. [29], in which strain is measured based on modulated power; its operating principle is quite different from that of other frequency-based SMS sensors.

In this work, by using Fresnel reflection at the distal open end of the MMF, we develop a single-end-access configuration of SMS-based strain and temperature sensing systems, in which PFGI-POFs were employed as MMFs to obtain high sensitivities. We experimentally show that when the MMF length is the same, the strain and temperature sensitivities do not largely change regardless of the configurations (i.e., either single- or two-end access).

2 Principle

A conceptual setup of the conventional two-end-access (or transmissive) configuration is depicted in Fig. 1(a). When light is injected from an SMF to an MMF, a few lower modes are excited in the MMF owing to the spot-size difference between the fundamental (or 0th) modes in the SMF and the MMF. They propagate along the MMF with their respective propagation constants and reach the other MMF-to-SMF interface, at which the net field coupled to the SMF is determined by the relative phase differences among the multiple modes guided in the MMF. Under the assumption that the MMF and SMFs are axially aligned, the modes excited in the MMF are axially symmetric, and the optical power P_{out} output from the SMS structure is expressed as [25]

$$P_{out} = |a_0{}^2 + a_1{}^2 \exp i(\beta_0 - \beta_1)L + a_2{}^2 \exp i(\beta_0 - \beta_2)L + \cdots|^2, \quad (1)$$

where a_i is the field amplitude of the i-th mode at the first SMF-to-MMF interface, β_i is the propagation constant of the i-th mode, and L is the MMF length. This equation indicates that the optical output power is influenced by physical changes (especially, the changes in the propagation constants and in the MMF length) caused by strain and temperature. Thus, by measuring the shift of spectral dips (or peaks), strain and temperature sensing can be performed.

Subsequently, a conceptual setup of the single-end-access (or reflectometric) configuration is shown in Fig. 1(b). The light injected from an SMF into an MMF via an optical circulator is Fresnel-reflected at the distal open end of the MMF and then propagates back along the MMF and the SMF; the output spectrum is

DOI: 10.1587/elex.14.20161239
Received December 14, 2016
Accepted December 16, 2016
Publicized January 13, 2017
Copyedited February 10, 2017

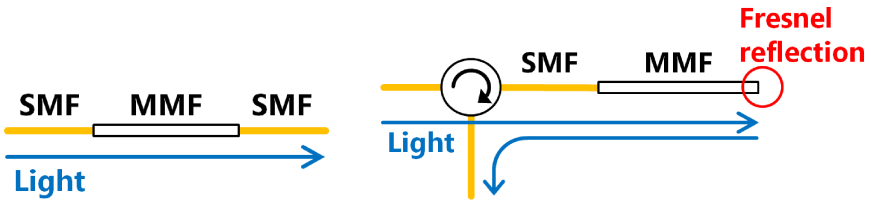

(a) (b)

Fig. 1. Conceptual setups of (a) transmissive configuration and (b) reflectometric configuration. MMF, multimode fiber; SMF, single-mode fiber.

finally observed at the third port of the circulator. In this reflectometric configuration, the optical path length in the MMF becomes twice as long as that in the transmissive one; the purpose of this work includes clarification of this effect on the sensitivities.

3 Experimental setup

The MMFs used in the experiment are PFGI-POFs [30] with a core diameter of 62.5 µm and a cladding diameter of 72.5 µm. Their core and cladding layers are composed of doped and undoped polyperfluorobutenylvinyl ether, respectively. The POF length is 0.7 m (except for the experiment of the length dependence measurement). The refractive indices at the center of the core and in the cladding layer are approximately 1.35 and 1.34, respectively, irrespective of the optical wavelength [31]. An overcladding layer (diameter: 750 µm) composed of polycarbonate is coated outside the cladding layer to lower microbending loss and to improve the load-bearing capability.

The actual experimental setups of transmissive (for comparison) and reflectometric configurations are shown in Fig. 2(a) and 2(b), respectively. In both configurations, a swept-source laser with a 20-kHz sweep rate was employed as a broadband light source with a central wavelength of 1320 nm and a bandwidth of 110 nm. The laser output was first input to a polarization controller to suppress the polarization-dependent spectral fluctuations, and then injected into the POF. In Fig. 2(a), both ends of the POF were butt-coupled to silica SMFs via "SC/PC-FC/PC" adaptors [32], and the spectrum of the transmitted light was monitored using an optical spectrum analyzer (OSA). In contrast, in Fig. 2(b), one end of the POF

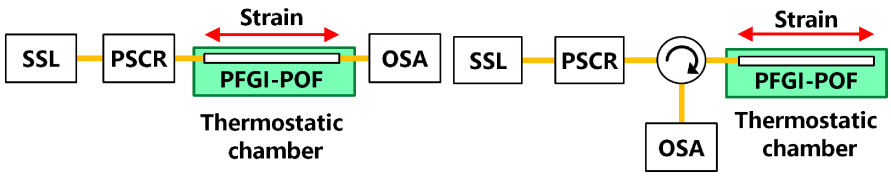

(a) (b)

Fig. 2. Actual experimental setups of (a) transmissive configuration and (b) reflectometric configuration. OSA, optical spectrum analyzer; PFGI-POF, perfluorinated graded-index polymer optical fiber; PSCR, polarization scrambler; SSL, swept-source laser. The yellow lines indicate silica single-mode fibers.

DOI: 10.1587/elex.14.20161239
Received December 14, 2016
Accepted December 16, 2016
Publicized January 13, 2017
Copyedited February 10, 2017

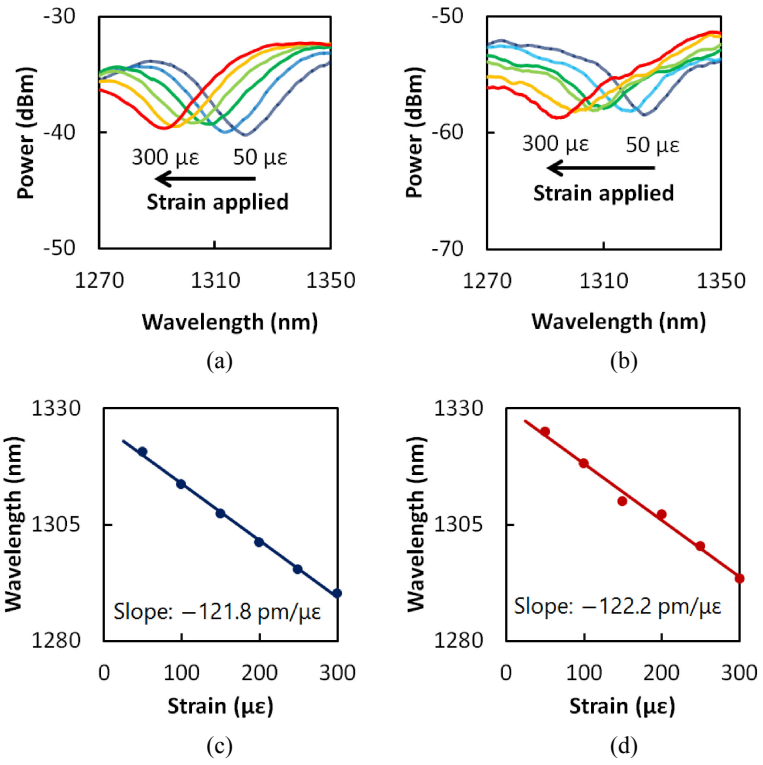

Fig. 3. Measured spectral dependences on strain in (a) transmissive configuration and (b) reflectometric configuration. The dip wavelength dependences on strain in (c) transmissive configuration and (d) reflectometric configuration.

was butt-coupled to a silica SMF in the same way, but the other end was kept open (flatly polished); the spectrum of the reflected light was monitored using an OSA. Note that the optical circulator used in Fig. 2(b) had an operating wavelength of 1280 to 1340 nm and insertion losses of approximately 0.5 dB for both directions (i.e., port 1 to port 2 and port 2 and port 3). In both cases, the entire length of the POF was strained or heated. The room temperature was approximately 28°C.

4 Experimental results

The measured dependences of the spectral dips on strain in transmissive and reflectometric configurations are shown in Fig. 3(a) and 3(b), respectively. In both cases, a single relatively broad dip was observed in this range, which shifted to shorter wavelengths with increasing applied strain. The spectral power in Fig. 3(b) was approximately 20 dB lower than that in Fig. 3(a); this is valid considering the loss of Fresnel reflection at the POF end (~2.2% reflection, corresponding to a 16.5 dB loss; by a simple calculation based only on the core refractive index difference) and the additional POF propagation loss (if compared with the Fresnel loss, negligibly low with this short POF (0.7 m)). In the reflectometric configuration, if necessary, we could form a mirror at the open end of the POF to increase the spectral power. Figs. 3(c) and 3(d) show the dip wavelengths plotted as functions of strain. The dependences were both almost linear with slopes of −1218 nm/% (= −121.8 pm/με; transmissive) and −1222 nm/% (= −122.2 pm/με; reflectometric). These values moderately agree with the previously reported

DOI: 10.1587/elex.14.20161239
Received December 14, 2016
Accepted December 16, 2016
Publicized January 13, 2017
Copyedited February 10, 2017

value [22]; the discrepancy probably originates from the imperfect end faces, asymmetric coupling to the SMFs, and longitudinal structural non-uniformity of the POF.

Subsequently, the dependences of the dip on temperature were also measured (Figs. 4(a) (transmissive) and 4(b) (reflectometric)). The dips shifted to shorter wavelengths as temperature increased. The dip wavelengths plotted as functions of temperature (Figs. 4(c) and 4(d)) indicate that the temperature-dependence coefficients were 9.63 nm/°C (transmissive) and 10.1 nm/°C (reflectometric); these values are also consistent with those previously reported [22]. Thus, the reflectometric configuration was experimentally proved to possess almost the same strain and temperature sensitivities as those of transmissive configuration with an advantage of single-end accessibility (see Appendix). One concern is that when the POF length is longer than several dozen meters, the additional propagation loss may result in the reflected spectrum buried by the noise floor. This problem could be mitigated by attaching a mirror at the end of the POF.

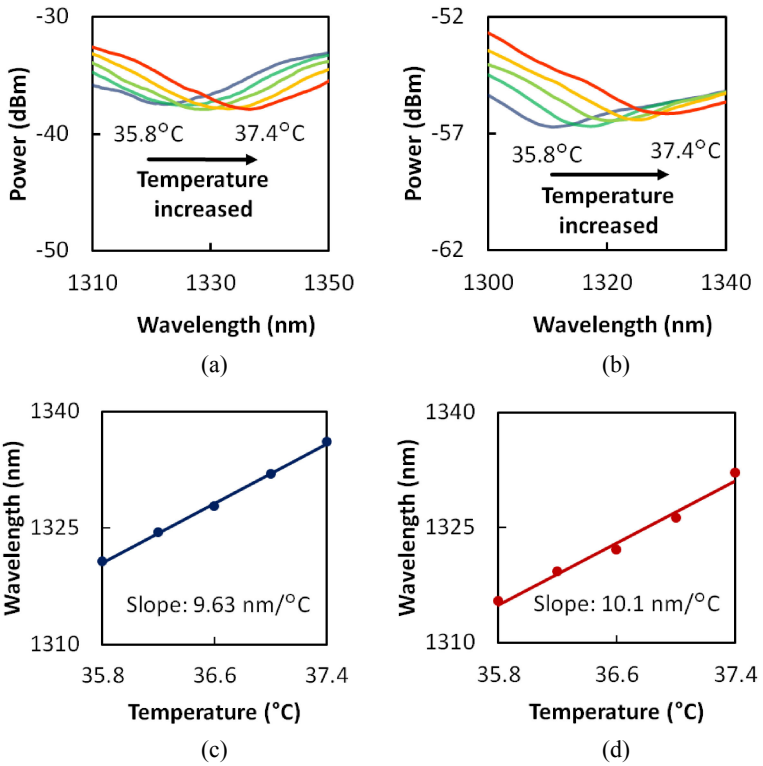

Fig. 4. Measured spectral dependences on temperature in (a) transmissive configuration and (b) reflectometric configuration. The dip wavelength dependences on temperature in (c) transmissive configuration and (d) reflectometric configuration.

5 Conclusion

A single-end-access configuration of SMS-based strain and temperature sensing systems exploiting Fresnel reflection at the distal open end of the MMF (PFGI-POF) was developed. High strain and temperature sensitivities of −122.2 pm/με

DOI: 10.1587/elex.14.20161239
Received December 14, 2016
Accepted December 16, 2016
Publicized January 13, 2017
Copyedited February 10, 2017

and 10.1 nm/°C, respectively, were obtained. These values were comparable to those in the two-end-access configuration. We anticipate that our method will drastically enhance the ease of handling of SMS-based fiber-optic sensors.

Acknowledgments

This work was supported by JSPS KAKENHI Grant Numbers 25709032, 26630180, and 25007652, and by research grants from the Japan Gas Association, the ESPEC Foundation for Global Environment Research and Technology, and the Association for Disaster Prevention Research.

Appendix

The experimental results may raise the question as to why, although the optical path length in the POF in the reflectometric configuration becomes twice the value in the transmissive configuration, the strain and temperature sensitivities are not doubled. This question leads to a fundamental discussion whether the strain and temperature sensitivities of SMS-based sensors are dependent on the MMF lengths or not.

Suppose the whole length of the MMF is strained or heated. As for the temperature sensitivity, in some references [20, 22, 23, 24], it was assumed to be in proportion to the MMF lengths and the units of "nm/°C/m", "pm/°C/cm", etc. were used, where the values expressed with "m" and "cm" are the MMF lengths. This way of using the units originates from the following theory: "for simplicity, suppose the interference of the lights only of the two modes (fundamental and first-order higher modes [24] or LP_{06} and LP_{07} modes [28]) propagating along the MMF. A longer MMF then leads to their longer optical-path difference (due to the thermal expansion, etc.), resulting in a larger temperature-dependence coefficient of the dip wavelength. Thus, the temperature sensitivity is linearly dependent on the MMF length". In the meantime, there has been a hot discussion on what units should be used for the strain sensitivity. In some references [20, 22, 23, 24], researchers used "pm/με", "nm/%", etc. probably considering that the strain sensitivity does not depend on the MMF length because strain in itself is the value divided by the MMF length. Nevertheless, from the standpoint of the aforementioned two-mode-interference theory, the induced optical path length difference between the two modes should be determined not by strain but by displacement. When the MMF is longer, larger displacement can be obtained with the same strain. Therefore, in this sense, the units for the strain sensitivity should be "pm/με/cm", "nm/%/m", etc.

However, if this conventional theory does hold true, our experimental results in the reflectometric configuration cannot be elucidated. To refute this theory, we measured the POF length dependences of the strain and temperature sensitivities, as shown in Figs. A1(a) and A1(b), respectively. POFs with lengths of 0.3, 0.7, 1.0, and 2.0 m were used. Although considerable fluctuations of the values probably caused by the modal instability were observed, it was clear that neither the strain sensitivity nor the temperature sensitivity was proportional to the POF lengths. This result indicates that in theoretical analysis of the performance of the SMS-based sensors, not only two modes but also many other modes need to be simultaneously considered. The details of the analysis is out of the scope of this paper, and will

DOI: 10.1587/elex.14.20161239
Received December 14, 2016
Accepted December 16, 2016
Publicized January 13, 2017
Copyedited February 10, 2017

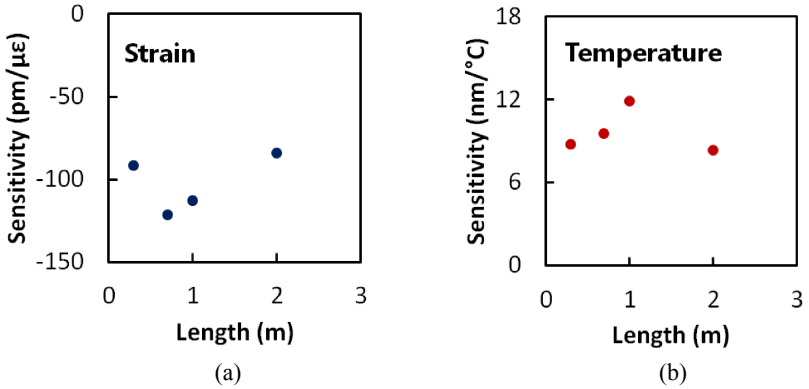

Fig. A1. Measured POF length dependences of (a) strain and (b) temperature sensitivities.

be discussed elsewhere. Hence, the practically important finding concerning the units is that we should use "pm/με", "nm/%", etc. for the strain sensitivity and "nm/°C", "pm/°C", etc. for the temperature sensitivity.

DOI: 10.1587/elex.14.20161239
Received December 14, 2016
Accepted December 16, 2016
Publicized January 13, 2017
Copyedited February 10, 2017